JPRS-UMS-93-004
21 June 1993

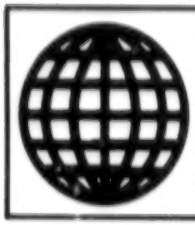

FOREIGN
BROADCAST
INFORMATION
SERVICE

JPRS Report

Science & Technology

Central Eurasia: Materials Science

Science & Technology
Central Eurasia: Materials Science

JPRS-UMS-93-004 21 June 1993

CONTENTS

Treatments

An Experimental Investigation of Effect of the Factors Existing in Outer Space on the Durability of Carbon Fiber-Reinforced Plastics. 1. Gas Release From Carbon Fiber-Reinforced Plastics in the Absence of Protective Coatings

937D0099C Moscow FIZIKA I KHIMIYA OBRABOTKI MATERIALOV in Russian No 1, Jan-Feb 93 (manuscript received 10 Jun 92) pp 47-54

[Article by I.A. Kulikov, A.A. Kupriy, F.G. Nichiporov, and G.A. Yurlova, Moscow; UDC 541.15]

[Abstract] The effects of different types of ionizing radiation (γ-radiation, electrons, protons, and α-particles) on freshly prepared and aged specimens of carbon fiber-reinforced plastic were compared. Flat test specimens of layered carbon fiber-reinforced plastics cut from LU-P-0.1 and LU-24P carbon strip and ENFB binder manufactured by the autoclave formation method and tube-shaped test specimens with an inner diameter of 49 mm, wall thickness of 3 mm, and length of 750 mm that had been produced from a carbon strip and binder by extrusion were used. The binder used in the tube-shaped specimens consisted of ED-20, EN-6, and SF-341A epoxy resins, UP-605/3 catalyst, furfurylglycide ether, polyethylene polyamine, and PN-609-21M polyester maleinate mixture. The binder used in the flat test specimens consisted of a mixture of EN-6 resin, the product EFU [not further identified], the catalyst UP 605/3, and SF-341A. The effects of the above types of radiation on gas release by the carbon fiber-reinforced plastic samples in different atmospheres (a vacuum, air, an inert atmosphere) and when exposed to treatment by thermal cycles (with a cycle extending from -150 to +120°C) were examined. The type of radiation did not affect the amount or composition of the gas released by the different test specimens. Treatment by thermal cycles resulted in a decrease in radiation-induced gas release from the carbon fiber-reinforced plastic samples. Figures 2, tables 3; references 14: 12 Russian, 2 Western.

An Experimental Investigation of Effect of the Factors Existing in Outer Space on the Durability of Carbon Fiber-Reinforced Plastics. 2. Special Features of Gas Release From Metallized Carbon Fiber-Reinforced Plastic

937D0099D Moscow FIZIKA I KHIMIYA OBRABOTKI MATERIALOV in Russian No 1, Jan-Feb 93 (manuscript received 10 Jun 92) pp 47-54

[Article by I.A. Kulikov, A.A. Kupriy, F.G. Nichiporov, and G.A. Yurlova, Moscow; UDC 541.15]

[Abstract] The effects of different types of γ-radiation and accelerated protons, treatment by thermal cycles, and preliminary moistening on gas emission from KMU-4L carbon fiber-reinforced plastic coated with with ultra-high-frequency reflective coatings were compared. The experiments examining radiation-induced gas release were performed with 5 x 5 x 1-mm carbon plastic specimens coated on with a reflective coating on both sides. A γ-dose rate of 1.5 Gy/s was used in the simultaneous irradiation and treatment by thermal cycles. The carbon plastic wafers tested on the proton accelerator measured 60 x 3 x 1 mm. They were placed in either vacuum- or gas-filled glass ampules and irradiated at a temperature of 20-25°C by accelerated protons with an initial energy of 18.5 MeV with a pulse-following frequency of 40 pulses/min and pulse duration of 8 μs. After the protons had passed through the front wall of the glass ampule, the proton energy was reduced to 10.5 MeV. The gas-release kinetics were monitored by the volumetric method or by connecting the ampules to a high-vacuum unit. The gas mixture's composition was determined chromatographically. Thin-film and foil versions of the reflective coating were compared. The foil coating cut radiation-induced gas release more than half under all of the different test conditions. The component composition of the gas released by the coated wafers remained virtually the same as that of noncoated irradiated wafers. Figures 3, tables 3; references 2: 1 Russian, 1 Western.

Carbon-Based Construction Materials for Thermonuclear Reactors and Their Radiation Resistance

937D0100A Moscow FIZIKA I KHIMIYA OBRABOTKI MATERIALOV in Russian No 2, Mar-Apr 93 (manuscript received 7 Aug 92) pp 5-21

[Article by Yu.S. Virgilyev, Graphite-Based Construction Materials Scientific Research Institute, Moscow; UDC 621.039.532.21]

[Abstract] Proper selection of construction materials for the primary wall, screens, diverter plates, and other structural components is one of the basic engineering problems involved in designing thermonuclear reactors with magnetic plasma confinement. The radiation-induced dimensional and physical changes occurring in the carbon-based construction materials produced in the former Soviet Union have been examined in the temperature range from 320 to 2,300 K under fluences up to 2×10^{22} neutrons/cm^2 ($E \geq 0.18$ MeV). The different types of construction materials developed in the CIS that are candidates for use in thermonuclear reactors may be grouped into five classes: fine-grained high-strength materials such as MPG; recrystallized boron-titanium-plated anisotropic graphites such as REKBOR, RG-B, RG-T, and GTM; carbon-based pyrocerams, which are pseudo-isotropic materials that are bulk-reinforced with a pyrocarbon structural skeleton (both with and without boron) such as USB-15 and PGI; highly anisotropic pyrolytic graphites (UPV-1, UPV-1T); and C-C composites such as KUP-VM, TERMAR-DV, GSP, and ARMIR. Studies have shown that graphite, the basis of the alloy-forming additives of carbide-forming elements (silicon, zirconium), does not cause any shape changes in the aforesaid reactor construction materials when such elements are used in amounts up to 10 percent. The growth of specimens in the range of secondary swelling (which reaches maximum speed at 1,000-1,100 K) has been found to cause an increase in porosity that reduces the above construction materials' strength properties and increases their thermal and electrical resistance. The possible existence of a high-temperature interval of radiation stability has been discovered. The heat conduction and resultant thermal stability of irradiated and untreated samples of the

study construction materials have been shown to differ little from one another at temperatures above 1,300 K. Studies have also shown that the structures of the study construction materials are rendered amorphous by irradiation with neutrons, electrons, and ions in rather high doses. USB-15 carbon-based pyroceram has been established to have a much higher radiation resistance than the other materials studied. The study construction materials have been found to have radiation resistance levels that are satisfactory from the standpoint of the performance conditions of the diverter plates of a physical model of a thermonuclear reactor. Figures 13, table 1; references 31: 29 Russian, 2 Western.

Effect of Metal + Ceramic Coatings on Fatigue Strength of Heat-Resistant Ni-Alloys

937D0083B Kiev PROBLEMY SPETSIALNOY ELEKTROMETALLURGII in Russian No 3, Jul-Sep 92 (manuscript received 27 Jan 92) pp 48-52

[Article by K.Yu. Yakobchuk, N.I. Korsakevich, V.A. Akrymov, and I.S. Malashenko, Institute of Electric Welding imeni Ye.O. Paton at Ukrainian Academy of Sciences, Kiev; UDC 669.187.526.001.5]

[Abstract] An experimental study of metal + ceramic composite coatings on three cast heat-resistant nickel alloys (ZhS6U, EI893 VD, ChS70VI) for blades of gas turbines and pistons of internal combustion engines was made. A ceramic ZrO_2 + 8 percent Y_2O_3 condensate overlayer protected a Ni-Cr-Al-Y or Co-Cr-Al-Y metal condensate underlayer against aggressive action of fuel combustion products. Some cylindrical specimens of each of the three alloys were left bare, some were coated with an 80 μm thick single Ni-Cr-Al-Y or Co-Cr-Al-Y layer only, and some of these were then additionally coated with a 50 μm thick ceramic overlayer. Having a 3 mm gage diameter and an 18 mm gage length, they were all tested for fatigue strength under symmetric tension-compression load cycles at room temperature (20°C), with a 184 Hz frequency of load alternation and a $30x10^6$ cycles test base. The test results and metallographic examination indicated that the outer ceramic layer with a columnar or crazing structure had not lowered the fatigue strength of ZhS6U specimens with a Ni-Cr-Al-Y coating and of EI893 VD specimens with a Co-Cr-Al-Y coating, the Co-Cr-Al-Y coating with a heterogeneous structure having lowered the fatigue strength because of its insufficient low-temperature plasticity. The fatigue strength of ChS70VI specimens was restored to that of bare specimens by prime coating them with a plastic monophase Co-Cr-Al-Y layer so as to inhibit fatigue cracking of the main Co-Cr-Al-Y layer under the ceramic one. Figures 4; references 14.

Electroplated Zinc Alloy-Based Diamond-Containing Coats

937D0104C Kiev SVERKHTVERDYYE MATERIALY in Russian No 2 (83), Mar-Apr 93 pp 41-43

[Article by I.A. Tsisar, G.N. Znamenskiy, A.P. Lobodzinskiy, Vinnitsa Polytechnic Institute; UDC 621.922.025:621.357.7]

[Abstract] The effect of such physical and mechanical properties of the binder as its viscosity, strength, and microhardness on the performance of diamond-containing tools on an electroplated base and the relationship between the electroplated binder hardness and the origin of the deposited metal and the electrolytic precipitation process are discussed, and the properties of composite diamond-containing electrochemical coats (KEP) on the basis of binary Zn alloys with Fe-group metals, i.e., Fe, Co, and Ni, are investigated. The alloys are produced using simple sulfate electrolytes. The polarization curves of Zn and its alloys using a Cl-Ag reference electrode and the dependence of the coat's microhardness on the current density are plotted. The resulting alloys make it possible to realize a gradual transition of properties from the soft binder to a hard one whereby an increase in the binder hardness makes it possible to secure the diamond grain and increase the grinding intensity. The use of grinding wheels with an electroplated Zn-Ni alloy base considerably improves the grinding efficiency; given the same grain size, the surface quality after grinding by corundum wheels from electrolytic alloys is higher than that produced by wheels made by powder metallurgy. The wheels made by the proposed method have been recommended for machining cutting inserts from synthetic corundum. The new technology is characterized by lower diamond powder and metallic matrix outlays. Figures 2; references 3.

Superplasticity of Ti6Al4V Structural Condensate Materials

937D0083A Kiev PROBLEMY SPETSIALNOY ELEKTROMETALLURGII in Russian No 3, Jul-Sep 92 (manuscript received 22 Apr 91) pp 44-48

[Article by A.V. Korzh and B.A. Movchan, Institute of Electric Welding imeni Ye.O. Paton at Ukrainian Academy of Sciences, Kiev; UDC 669.187.526.001.2]

[Abstract] An experimental study of the Ti6Al4V alloy with addition of ZrB_2 was made, this refractory additive serving as an excellent agent for control of structural and mechanical characteristics. As raw materials industrial-grade V-Ti6 alloy and pure ZrB_2 powder were used. Specimens with 0.25-7 percent ZrB_2 were produced by electron-beam evaporation and vacuum condensation on a substrate, macrocrystalline and microcrystalline condensates being obtained by appropriately different processing cycles in the experimental UE-366 apparatus. Heavy about 7 mm thick and about 500 mm in diameter microcrystalline condensate with the optimum ZrB_2 content was obtained in the experimental UE-193M apparatus. Structural examination under a Polyvar-Met optical microscope and under a JSEM-200 emission electron microscope revealed that addition of ZrB_2 had decreased the grain size: in macrocrystalline (α+β)-phase condensates from 12 mm to 3 mm and in microcrystalline predominantly α-phase condensates from 0.9-1.1 mm (about 0.25 percent ZrB_2) to 0.4 μm (0.45+ percent ZrB_2. Flat specimens were tested in tension at a strain rate of 0.0017 s^{-1} at temperatures covering the 20-600°C range. Measurements of 0.2 percent yield strength, ultimate strength, and percentage elongation revealed a nonmonotonic dependence of these mechanical characteristics on the ZrB_2 content, the plasticity peaking to a maximum within the range of low ZrB_2 content and the microcrystalline condensates being stronger and less plastic than the macrocrystalline ones. They revealed, moreover, superplasticity of microcrystalline condensates with 0.35-1.8 percent ZrB_2 , the elongation having increased from 6 percent (0.35 percent ZrB_2) at 20°C test temperature to about 150 percent at 500°C and to about 600 percent at 600°C. Annealing at 1000°C under vacuum for two hours enlarged the grain size to about 80 mm, the grains then consisting then colonies of parallel 1-4 μm thick α-phase lamellae separated by β-phase intercalations. Such an annealing thus canceled the superplasticity of microcrystalline condensates, restoring their mechanical characteristics to those of plain V-Ti6 alloy. Figures 5; references 3.

Thermal Conductivity of Diamond Compacts With Co_3C Content

937D0084A Kiev SVERKHTVERDYYE MATERIALY in Russian No 6, Nov-Dec 92 (manuscript received 11 Dec 91, final version received 17 Apr 92) pp 9-12

[Article by O.A. Voronov and Ye.S. Chebotareva, Institute of High-Pressure Physics at Russian Academy of Sciences, Troitsk (Moscow Oblast); UDC 679.826.002.2]

[Abstract] The thermal conductivity of polycrystalline diamond powder compacts containing cobalt carbide was measured at room temperature, for a determination of its dependence on the grain size and for a comparison with that of pure compacts. Diamond powders were produced by crushing 1.0-1.2 mm large single crystals from the Yakutsk kimberlite deposits and then segregated into 630-500, 500-350, 350-200, 200-100, 80-63, 63-50, 20-10 μm grain size fractions by passage through sieves. After they had been washed in boiling acids, they were mixed with 10 wt. percent of PK1 fine-disperse cobalt powder. The total content of noncombustible impurities did not exceed 0.2 wt. percent. The powder mixtures were compacted to 3.5-3.7 g/cm^3 density by being held for 10-20 seconds in a toroidal apparatus under a pressure of 8.9-9.0 GPa at a temperature within the 1400-1600°C range. From these compacts were, with an LTI-502 laser, cut out 3.0 mm long cylinders 3.5 mm in diameter. These were polished with diamond micropowder and then etched with aqua regia at room temperature for removal of surface impurities. Chemical analysis of the compacts was performed in an X-ray diffractometer and under a scanning electron microscope with microanalyzer. Some compacts were then calcined in air at 900°C for eight hours, sufficiently long for burning out the free carbon so that the second component could be examined. All the cobalt was found to have reacted with carbon, and the carbide with a structure similar to that of Fe_3C to have precipitated in micropores only and thus not inhibited the growth of diamond grains. The thermal conductivity of these compacts was measured at room temperature by the constant thermal flux method, accurately within 10 percent. Its dependence on the grain size was found to be nonmonotonic: increasing from 220 W/(m.K) (20 μm grains) to 440 W/(m.K) (63 μm grains), then decreasing to 190 W/(m.K) (350 μm grains), then again increasing to 320 W/(m.K) (600 μm grains) and thus remaining lower than the thermal conductivity of pure diamond compacts within the 100-600 μm grain size range. The decrease of thermal conductivity with increase of the grain size from 63 μm to 350 μm is evidently due to fracture of larger grains and formation of additional defects as well as due to enlargement of the overall diamond-carbide contact area. The subsequent increase of thermal conductivity with further increase of the grain size to 600 μm is due to a changing balance between two counteracting processes: increase of the grain size and decrease of the overall direct diamond-diamond contact area. The mechanism of compact formation and some physical properties (mechanical strength up to 4.0 GPa, electrical resistivity up 10 Mohm.cm) of these compacts are similar to those of pure diamond compacts. The authors thank V.V. Pimenov, N.F. Borovik, Ye.P. Zhlybov, and L.F. Afanasyeva for constant assistance. Figures 2; references 5.

Characteristics of TiN-(Ni, Mo) Cermet Structure Formation

937D0084B Kiev SVERKHTVERDYYE MATERIALY in Russian No 6, Nov-Dec 92 (manuscript received 18 Mar 92) pp 24-29

[Article by M.A. Kuzenkova, O.N. Kaydash, L.M. Yupko, and V.V. Shumeyko, Institute of Superhard Materials at Ukrainian Academy of Sciences, Kiev; UDC 621.762]

[Abstract] An experimental study of liquid-phase sintering of $TiN_{0.84}$-(Ni, Mo) cermets was made, with molybdenum in a Mo:Ni = 1:3 ratio added to the nickel binder melt so as to improve wetting of the $TiN_{0.84}$ filler powder. Sintering was done under vacuum and in a nitrogen atmosphere at temperatures covering the 800-1900°C range, the Ni content being varied over the 10-40 percent range and the process being completed in 30 minutes under all conditions. The cermets were subjected to structural examination under a Neophot-2.0 optical microscope, structural and phase analysis in a DRON-30 X-ray diffractometer, differential thermal analysis in a VDTA-7 apparatus, and X-ray spectrum microanalysis in a Camscan-5. The results indicate how the composition of cermets and of $TiN_{0.84}$ grains with impurity inclusions depend on the sintering temperature. They indicate formation of a ring structure on grains of that refractory component, whether under vacuum or in a nitrogen atmosphere. Heating to 800°C led to formation of Mo_2C carbide. Further heating accelerated a solid-phase interaction during which up to 15 percent of the molybdenum (from its carbide) and up to 6 percent of the titanium dissolved in the nickel. During sintering at 1200°C, it had also formed traces of the Ni_3Mo intermetallic compound. Endothermal reactions took place at 1330°C and 1390degC, nonhomogeneity of the Ni-Mo binder phase causing melting to take place in two stages. Repeated heating evidently homogenized it, inasmuch as it lowered its end-of-melting temperature. Figures 5; tables 3; references 12.

Effect of Laser Treatment on Strength of Powder of Synthetic Diamonds

937D0084C Kiev SVERKHTVERDYYE MATERIALY in Russian No 6, Nov-Dec 92 (manuscript received 12 May 92, final version received 21 Aug 92) pp 32-32

[Article by G.P. Bogatyreva and G.A. Bazaliy, Institute of Superhard Materials at Ukrainian Academy of Sciences, Kiev; UDC 535.211]

[Abstract] Hardening of high-strength synthetic diamond powder by laser treatment was studied in an experiment with powder of the 400-315 μm grain size fraction. Powder of this fraction was segregated into 12 powder specimens according to the degree of grain defectiveness on the basis three indicators: magnetic susceptibility χ indicating the degree of internal defectiveness, electrical resistivity ρ indicating the degree of surface defectiveness, and dielectric loss tangent tan δ indicating the degree of total defectiveness (smaller tan δ, lower χ, and higher ρ characterizing less defective diamond grains). In addition the breaking load for grains of each powder was also determined. The energy density of laser treatment was varied: 1) over the 9-12 J/cm^2 range for a group of four powders, 2) over the 14-20 J/cm^2 range for a group of three powders, 3) over the 30-50 J/cm^2 range for a group of five powders. The results indicate that

laser treatment with a certain energy density hardened most the powder of least defective grains. Considering that treatment with an excessive energy density can evaporate the surface layer and that the energy density can be controlled by varying the laser power and the exposure time, special tests were performed for the purpose of determining how the mechanical properties of the diamond powders depended on these two parameters. These tests were performed on five powders representing all three groups. They were performed in two ways: with constant radiation intensity and with constant exposure time. The results of these tests indicate that for each powder there exists optimum ranges of radiation intensity, exposure time, and energy density. They also indicate that the powder with most surface defects (minimum electrical resistivity) should have been treated with lower radiation intensity for a longer time and the powder with most overall defects (maximum dielectric loss tangent) should not have been laser treated at all. Tables 1.

Refining Vanadium-Alloy Tailings With Vanadium Content by Remelting

937D0083C Kiev PROBLEMY SPETSIALNOY ELEKTROMETALLURGII in Russian No 3, Jul-Sep 92 (manuscript received 10 Jul 91) pp 80-83

[Article by I.V. Sheyko, Yu.V. Latash, G.A. Vysotskiy, V.V. Stepanenko, A.A. Dolomanov, Yu.A. Lukyanichev, B.Ya. Tadzhiyev, and O.G. Yegorov, Institute of Electric Welding imeni Ye.O. Paton at Ukrainian Academy of Sciences, Kiev; State Institute of Rare Metals, Moscow; Leninabad Rare Metals Combine; UDC 669.187.58]

[Abstract] An experimental feasibility study was made concerning use of a sectional crystallizer for refining vanadium-alloy tailings with vanadium content by remelting them, tailings of the V-Al-Ti alloy (50.89 percent V, 40.18 percent Al, 6.9 percent Ti, and 2.1 percent C) produced by the Leninabad Combine being contaminated mainly by Al_2O_3 but also other oxides and carbides along with other nonmetallic inclusions (0.58 percent Fe, 0.20 percent Cu, 0.31 percent Si, and 0.200-0.230 percent [O]). Melts were produced in an inert argon atmosphere under a pressure of 0.11-0.12 MPa in an electric induction-type 8 kHz laboratory crystallizer with a 100 mm large diameter. Melting was done with addition of 2 percent CaF_2 flux per ingot and also without flux. Addition of flux to the melt was found to result in formation of an up to 1 mm thick skin layer of slag around the lateral surface of ingots, this skin layer while still in the liquid state having effectively assimilated ascending nonmetallic inclusions. Structural examination revealed no shrinkage and porosity defects. Chemical analysis revealed no significant change of alloy composition (50.60 percent V, 40.18 percent Al, 6.8 percent Ti, and 2.1 percent C) and an appreciable decrease of impurities (0.33 percent Fe, 0.09 percent Cu, 0.27 percent Si, and 0.025-0.026 percent [O]. Figures 3; tables 1; references 3.

The Structure and Electro-Optical Properties of $Cu_{0.33}In_{1.67}S_3$ Monocrystals

937D0096A Moscow NEORGANICHESKIYE MATERIALY in Russian Vol 29 No 4, Apr 93 (manuscript received 21 Apr 92) pp 483-485

[Article by G.G. Guseynov, I.G. Aliyev, S.S. Rzayev, O.M. Aliyev, and F.I. Aliyev, Physics Institute, Azerbaijan Academy of Sciences; UDC 548.3;621.315.592]

[Abstract] The structure and electrooptical properties of monocrystals based on the ordered phase In_2Se_3 with partial replacement of the tetrahedrally coordinated in atoms by Cu were studied. The $Cu_{0.33}In_{1.67}S_3$ crystals were synthesized by heating the starting mixture in a single-temperature furnace to 1,050°C at a rate of 100°/min, holding the mixture for half an hour, cooling it slowly to 400°C, and holding it at that temperature for 150 hours. The crystals had the following elementary cell parameters: a = 15.63 angstroms; c = 18.95 angstroms; c/a = 1.21; limiting boundary, $P6_3$; and Z = 32. A phase with a structure similar to the structure of α-In_2Se_3 was thus produced. Volt-ampere and optical studies of the crystals demonstrated that $Cu_{0.33}In_{1.67}S_3$ is a semiconductor with a forbidden band width (E_g) of 1.47 eV. The studies further established that films of the new crystal deposited on the surface of NaCl substrates are amorphous at room temperature but polycrystalline with a sphalerite-based ordered structure (a = 11.2 angstroms) at 150°C. At temperatures above 200°C, a face-centered crystal phase (a = 5.45 angstroms with a sphalerite structure is formed. Figures 3, table 1; references 2: Russian.

Alloys of Chromium With Cerium and Lanthanum Monosulfides

937D0096B Moscow NEORGANICHESKIYE MATERIALY in Russian Vol 29 No 4, Apr 93 (manuscript received 23 Apr 92) pp 486-488

[Article by G.P. Dmitriyeva, A.K. Shurin, and A.V. Chernogorenko, Metal Physics Institute, Ukraine Academy of Sciences; UDC 669.017.13.26'855'755']

[Abstract] Cr-CeS and Cr-LaS alloys corresponding to the ternary systems Cr-Ce-S and Cr-La-S were subjected to metallographic, differential thermal, and X-ray phase analyses (with a Neophot-2 optical microscope, VDTA-80M differential thermal analyzer, and DRON-UMI diffractometer, respectively). The studies established that the fusibility curve of the section Cr-CeS of the system Cr-Ce-S is characterized by the presence of a region of immiscibility in the liquid state in the concentration range from 4 to about 50 mass percent CeS. The curve contains two regions of primary crystallization. At 1,760°C the system Cr-CeS is characterized by a monotectic reaction; at 970°C, it is characterized by a eutectic reaction. The fusibility curve of the section Cr-LaS of the system Cr-La-S contains a region of immiscibility in the liquid state in the concentration range from 4 to about 50 mass percent LaS and a eutectic point at 1,000°C. At that point the LaS content does not exceed 60 percent. Figures 2; references 5: 4 Russian, 1 Western.

Ln_2O_2S-Sb_2S_3 (Ln = La, Ce, Pr) Systems

937D0096C Moscow NEORGANICHESKIYE MATERIALY in Russian Vol 29 No 4, Apr 93 (manuscript received 30 Jun 92) pp 489-491

[Article by O.M. Aliyev, V.S. Tanryverdiyev, and I.I. Aliyev, Inorganic and Physical Chemistry Institute, Azerbaijan Academy of Sciences; UDC 546.65'21'22+863'22]

[Abstract] A study examined the reactions occurring in the systems Ln_2O_2S-Sb_2S_3 (where Ln = La, Ce, and Pr). The study alloys were synthesized from Ln_2O_2S and Sb_2S_3 in single-section furnaces at 1,050-1,100°C. The melts were held at those temperatures for three hours, stirred intensively, and then cooled slowly to 600°C. The alloys were then annealed at the specified temperatures for 240 hours to homogenize them. Their homogeneity was controlled by differential thermal analysis, X-ray phase analysis, and microstructural analysis. The systems Ln_2O_2S-Sb_2S_3 were found to be quasi-binary. The liquidus of each system was characterized by five primary phase separation arms: Ln_2O_2S, $(LnO)_4Sb_2S_5$, $LnSbOS_2$, $LnSb_3OS_5$, and Sb_2S_3. A study of the alloys synthesized through 5 molecular percent indicated that three compounds form in the system, i.e., $(LnO)_4Sb_2S_5$, $LnSbOS_2$, and $LnSb_3OS_5$. All of them formed in accordance with peritectic reactions. The peritectic reactions in the system containing La occurred at 825, 715, and 600°C; those in the system containing Ce occurred at 835,

730, and 605°C; and those in the system containing Pr occurred at 815, 700, and 635°C. The compounds $(LnO)_4Sb_2S_5$ and $LnSbOS_2$ were found to crystallize in a tetragonal singony. The eutectic of the system containing La contained 12 molecular percent La_2O_2S and melted at 430°C, that of the system containing Ce contained 18 molecular percent Ce_2O_2S and melted at 460°C, and that of the system containing Pr contained 16 molecular percent Pr_2O_2S and melted at 445°C. Figures 3; references 6: 4 Russian, 2 Western.

An Investigation of Solid Alloys Based on Titanium-Molybdenum Carbide Produced by the Method of Self-Propagated High-Temperature Synthesis

937D0096D Moscow NEORGANICHESKIYE MATERIALY in Russian Vol 29 No 4, Apr 93 (manuscript received 28 May 92) pp 510-513

[Article by V.M. Bunin, I.P. Borovinskaya, L.F. Mikulinskaya, and A.Ye. Sychev; UDC 54-172]

[Abstract] Three carbides were produced from solid titanium-molybdenum solutions synthesized by the method of self-propagated high-temperature synthesis. The solutions had in turn been produced from titanium obtained by calcium hydride reduction of TiO_2, hydrogen-reduced molybdenum, and PM-15 TC black. The alloys produced were as follows: $Ti_{0.93}Mo_{0.07}C_{0.95}$, $Ti_{0.95}Mo_{0.05}C_{0.95}$, and $Ti_{0.97}Mo_{0.03}C_{0.95}$. Studies performed on the new alloys established that $Ti_{0.93}Mo_{0.07}C_{0.95}$ has a hardness of 91.5 to 91.9 HRA and bending strength of 1,010 to 1,270 MPa, $Ti_{0.95}Mo_{0.05}C_{0.95}$ has a hardness of 92.3 to 92.7 HRA and a bending strength of 1,420 to 1,520 MPa, and $Ti_{0.97}Mo_{0.03}C_{0.95}$ has a hardness of 92.2 to 92.4 and a bending strength of 1,400 to 1,800. The new alloys were found to have acceptable cutting properties and to be suitable for use in the accessories of a DO-137A press unit set up to produce type AS-2 diamonds. Figures 4, tables 3; references 4: Russian.

Isothermal Sections of the Systems HfO_2-Y_2O_3-CaO and ZrO_2-Y_2O_3 at 1,100°C

937D0096E Moscow NEORGANICHESKIYE MATERIALY in Russian Vol 29 No 4, Apr 93 (manuscript received 21 May 92) pp 530-534

[Article by Ye.R. Andriyevskaya, L.M. Lapato, and I.Ye. Kiryakova, Materials Science Problems Institute imeni I.N. Frantsevich, Ukraine Academy of Sciences; UDC 546.651/659]

[Abstract] The reactions occurring in the systems HfO_2-Y_2O_3-CaO and ZrO_2-Y_2O_3 at 1,100°C were studied. Isothermal sections of their phase diagrams were plotted. The study systems were found to be characterized by the formation of regions of homogeneity based on *M*- and *F*-modifications of HfO_2; *M*-, *T*-, and *F*-modifications of ZrO_2, CaO, and C-Y_2O_3; and the compounds $Ca_2Hf_7O_{16}$, $CaZr_4O_9$, $Ca_6Zr_{19}O_{44}$, $CaHfO_3$, and $CaZrO_3$. No region of homogeneity based on the δ-phase ($Zr_3Y_4O_{12}$) was detected in the ternary system ZrO_2-Y_2O_3-CaO. Figure 1, tables 2; references 23: 4 Russian, 19 Western.

Vacuum Ultraviolet Radiation-Stimulated Creep of Selected Polymeric Materials

937D0099B Moscow FIZIKA I KHIMIYA OBRABOTKI MATERIALOV in Russian No 1, Jan-Feb 93 (manuscript received 2 Jun 92) pp 39-46

[Article by V.V. Abraimov, K.Sh. Bocharov, I.V. Budnyak, and V.V. Danovskiy, Kharkov; UDC 687.019.63:539.3]

[Abstract] A study examined the effects of vacuum ultraviolet radiation-stimulated creep in three polymeric materials: polyethylene, Teflon, and polyethylene terephthalate. A special simulator was developed for the study. A GIS-1 gas stream light source was used to simulate the Sun's electromagnetic radiation in the vacuum UV range (λ = 5 to 200 nm). The study polymeric materials were deformed by the method of gradual loading in increments of 2 to 3 x 10^{-2} N. Each successive load induced macroscopic creep in the study materials. The deformation was measured by an inductive sensor with a sensitivity of $\Delta l/l_0 = 10^{-6}$, and a KSP-4 automatic recorder was used to record the elongation. Films of the three polymers in the form of two-sided vanes measuring 20 mm in length, 5-10 mm in width, and 20 to 100 μm in thickness were used. The courses of the deformation curves plotted for each material turned out to be identical and were characterized by a significant increase in the plastic deformation rate at the moment when the vacuum UV radiation began. This plastic deformation-stimulating effect of the VUV radiation was reversible. The stimulation of plastic deformation observed was found to be associated not with the thermal component of the VUV radiation but rather with the occurrence of radiation defects, which were in turn apparently linked to the destruction of molecular and intermolecular bonds under the effect of quanta of vacuum ultraviolet. It was hypothesized that the radiation defects diffuse from a narrow surface layer of polymer film (where they are generated) into the bulk of the test specimens, thus causing a macroscopy change in the plastic deformation rate. The results obtained were discussed in terms of the theory of VUV-stimulated creep proposed by A.M. Kosevich and A.I. Landau. Figures 5; references 9: Russian.

The Convective Mechanism of Liquid-Phase Alloying of Metals' Surface During a Pulsed Plasma Effect

937D0099E Moscow FIZIKA I KHIMIYA OBRABOTKI MATERIALOV in Russian No 1, Jan-Feb 93 (manuscript received 22 Jun 92) pp 59-66

[Article by Ye.A. Budovskikh, V.D. Sarychev, V.P. Simakov, and P.S. Nosarev, Novokuznetsk; UDC 669.295.69:621.793]

[Abstract] The mechanism of convective alloying of the liquid-phase surface layers of metals formed by pulsed plasma jets was studied. Heterogeneous plasma beams were produced by exploding a carbon-graphite textile. Samples of a number of metals with different chemical activities with respect to carbon (i.e., titanium, iron, nickel, and copper) were treated for the sake of comparison. Metallographic studies (by a light microscope) of etched polished specimens indicated that the alloying occurred throughout the entire depth of the fused layer. In low-energy modes, condensed particles from the back of the beam of explosion products condensed on the metals' surface in the form of finely

dispersed fragments of carbon-graphite fiber and formed a coating that did not penetrate the melt. The alloying was accomplished by the vapor-plasma component of the beam. When the beam's parameters were increased, the condensed particles also contributed to the alloying of the titanium and iron. When the surface layer crystallized, the carbon dissolved in the melt resulted in the formation of solid solutions, TiC and Fe_3C carbides, and globules of graphite in the copper. When the beam interacted with the melt, the plasma-metal interface surface became unstable and resulted in the formation of surface periodic structures. A possible mechanism of plasma alloying was considered. The mechanism entailed adsorption of ionized carbon on the surface of the melt and mixing of the carbon into the bulk of the liquid layer by convective flows linked to the surface periodic structures. Calculations performed indicated that the relative role of heat and mass transfer in the liquid layer due to convection is greater than that of heat conduction and diffusion. Figures 2, tables 3; references 20: Russian.

The Damage Susceptibility of Vanadium-Titanium Alloys Subjected to Pulsed Laser Radiation in a Vacuum

937D0100B Moscow FIZIKA I KHIMIYA OBRABOTKI MATERIALOV in Russian No 2, Mar-Apr 93 (manuscript received 29 Sep 92) pp 42-48

[Article by S.A. Maslyayev, V.I. Neverov, V.N. Pimenov, Yu.M. Platov, S.Ya. Betsofen, and I.P. Sasinovskaya, Metallurgy Institute imeni A.A. Baykov, Russian Academy of Sciences, Moscow; UDC 621.71]

[Abstract] Two vanadium-titanium alloys were subjected to the effects of the pulsed radiation of a laser operating in a free-lasing mode. The first alloy consisted of vanadium and 10 atomic percent titanium, and the second alloy consisted of vanadium and 35 atomic percent titanium. The O, N, H, and C impurities in the alloys did not exceed 0.04 mass percent in toto. The study alloy specimens were produced by cold rolling to a thickness of about 1 mm and were annealed in a vacuum with a residual pressure of about 1×10^{-4} Pa at 1,273 K for an hour prior to irradiation. The study specimens were irradiated at an intensity of 2,600 MW/m^2 with a pulse duration of 0.7×10^{-3} s. This irradiation regimen resulted in meltdown of the specimens' near-surface layers, vaporization of their components, and rapid liquid-phase crystallization. No cracking of either alloy was noted. The process of vaporization of the alloys' components in a vacuum when subjected to a laser pulse was very intensive (with a characteristic speed on the order of 1 cm/s). The macrostructure of the study alloys' near-surface layers after "laser hardening" was found to correspond to the process of directed crystallization of a melt to the seed and to reproduce the initial crystllographic orientation of the grains in the irradiated plane of the specimen. The crystallization texture of a β (V, Ti)-solution in the direction of the temperature gradient after a laser radiation effect remained unchanged from the starting texture. Somewhat of a decrease in the lattice parameter of the β (V, Ti)-solution occurred in the recrystallized layers of the irradiated alloys in the direction of the normal to the irradiation plane. This decrease was linked to the effect of the residual tensile macrostresses occurring on the specimens' surfaces after the effect of the laser pulse. A microinhomogeneity of the lattice of the said solution that was more noticeable than in the starting specimens was established. Figures 2, table 1; references 17: 8 Russian, 9 Western.

Immobilization of Sulfate-Containing Radioactive Wastes in Glass

937D0100D Moscow FIZIKA I KHIMIYA OBRABOTKI MATERIALOV in Russian No 2, Mar-Apr 93 (manuscript received 10 Apr 92) pp 63-77

[Article by S.V. Stefanovskiy, Radon Scientific Production Association, Moscow; UDC 621.039.73]

[Abstract] A study examined the principal problems involved in immobilizing sulfate-containing radioactive waste in glass. The study glass was synthesized under laboratory and pilot-commercial conditions in a silicon carbide furnace at temperatures up to 1,200°C. Glass with the optimal composition was produced in pilot units based on a ceramic melter with resistance (Joule) heating or an induction melter with a cold crucible. The melts were poured into carbon steel containers. Between 25 and 30 kg of glass with a volume of about 0.01 m^3 was poured into each. The glass samples were subjected to chemical analysis. Samples of glass containing actual radioactive waste were subjected to radiochemical measurements to determine the coefficient of the distribution of radionuclides between the sulfate phase and glass phase. The structure of the glass was studied by infrared spectroscopy, electron paramagnetic resonance, X-ray phase analysis, and electron microscopy. The rate of leaching of radionuclides from the samples was determined by the International Atomic Energy Agency method, density was determined by hydrostatic weighing in water or toluene, and radiation resistance was determined from the change in the samples' leaching rate after γ-irradiation to a dose of 10^6 Gy by a ^{60}C source. The study confirmed that it is, in principle, possible to create silicate-, borosilicate-, and phosphate-based glass suitable for immobilizing sulfate-containing radioactive waste. Sulfate ions may be dissolved in different types of glass in different amounts while still retaining a chemical stability meeting the requirements set for solidification of radioactive waste. These amounts are as follows: 10 to 15 percent in cases of aluminum, zinc, iron, and lead phosphate glass; 5 to 7 percent in cases of lead and vanadium silicate or borosilicate glass; and 3 to 4 percent in cases of high-alkaline silicate and aluminosilicate glass. In the structure of glass based on silicate, borosilicate, or meta- and pyroaluminophosphate, the sulfate ions occupy vacancies in the lattice and remain essentially autonomous. Partial losses of sulfur oxides occur when sulfate-containing radioactive wastes are fixed in glass. High process temperatures and high amounts of reducing agents are associated with higher sulfur oxide losses. The amount of off gases generated does not increase greatly, and the sulfate decomposition products do not contain carriers of radioactivity (the sulfur and oxygen isotopes are stable). The main drawback of sulfate-containing glass is its high corrosion activity with respect to aluminosilicate and baddeleyite-corundum refractories. This problem may be overcome by using a skull induction melter with a cold crucible as the melting unit. Melters with plasma heating also appear promising. Figure 1, tables 8; references 41: 34 Russian, 7 Western.

The Use of High-Voltage Glow Discharge To Test Selected Materials Used in Thermonuclear Reactors

937D0100E Moscow FIZIKA I KHIMIYA OBRABOTKI MATERIALOV in Russian No 2, Mar-Apr 93 (manuscript received 27 Jul 92) pp 92-99

[Article by Ya.Ya. Udris, All-Russia Electrical Engineering Institute imeni V.I. Lenin, Moscow; UDC 621.739.7]

[Abstract] Preliminary research demonstrated that a strong high-voltage glow discharge can provide good simultaneous simulation of a number of the effects that plasma exerts on the primary wall and diverter of a thermonuclear reactor. These effects include the following: high-density release of heat from the heat flux; irradiation by fast particles (excluding neutrons); cathode sputtering; erosion of unipolar arcs by cathode spots; and radiation blistering. These findings led to the proposal of a new comprehensive method of testing materials that interact with plasma in a thermonuclear reactor. The new method was based on the use of high-power electron guns whose cathodes were made of the material being tested. During the course of the experiments conducted to test the new high-voltage glow discharge method, researchers achieved a heat flux density of about 1 kW/cm^2 on aluminum and its alloys, an irradiation intensity on the order of $10^{18}/cm^2/s$, and an arc cathode spot erosion corresponding to the passage of more than 10^4-10^5 C of electricity. The tests confirmed that it will be possible to achieve an unlimited increase in density of the heat flux onto a material undergoing testing (i.e., cathode) by means of a high-voltage glow discharge once the required special test devices have been developed. Figures 4, table 1; references 16: 12 Russian, 4 Western.

Sintering Kinetics of Natural Diamond Crystals in Metamorphic Rock

937D0104A Kiev SVERKHTVERDYYE MATERIALY in Russian No 2 (83), Mar-Apr 93 pp 3-6

[Article by O.A. Voronov, A.A. Kaurov, High Pressure Physics Institute at Russia's Academy of Sciences, Troitsk, Moscow oblast; UDC 621.921.27]

[Abstract] The polycrystal formation at high pressures and temperatures from synthetic and natural diamond powders extracted from metamorphic rock is discussed, and it is noted that both volcanic and metamorphic rocks may contain a large quantity of industrial diamonds (bort). The sintering kinetics of natural diamond crystals from metamorphic rock is investigated. To this end, the initial diamond powder with a 10-20 μm grain size is processed in hydrofluoric and hydrochloric acid after which the ash content does not exceed 0.1 percent by mass; the samples are produced in a toroidal device with a 15 mm indentation diameter at an initial 8 GPa pressure. The dependence of the wear rate of the compacts sintered from diamond powder with a 10-20 μm grain diameter on the sintering parameters at an 8 GPa pressure during grinding by a silicon carbide wheel is plotted, and the (331) and (220) diffraction peak width of the diamond lattice under the effect of various temperatures and pressures on the diamond powder is measured under different powder processing conditions. The X-ray phase study reveals a considerable broadening of the diffraction peaks during the powder sintering. The diamond grain intergrowth occurs by means of diffusion in the contact areas at a 1,300-2,200°C temperature whereby the diffusion intergrowth rate largely depends on temperature which is manifested by the dependence of the abrasion resistance on the exposure duration. The intergrowth is accompanied by a decrease in resistivity. A Vickers estimate of the sintered diamond microhardness shows that the mean pressure under the indentor during the experiment is equal to 59-74 GPa at a wear rate of up to 0.5-0.9 mm^3/min. Figures 1; tables 1; references 6.

Graphite Wettability by Ni-Mo and Ni-W Melts and Their Contact Interaction

937D0104B Kiev SVERKHTVERDYYE MATERIALY in Russian No 2 (83), Mar-Apr 93 pp 6-11

[Article by V.M. Perevertaylo, O.B. Loginova, A.V. Gorbach, Superhard Materials Institute at the Ukrainian Academy of Sciences, Kiev; UDC 539.219.3:620.18]

[Abstract] Production of carbon-based composites with multicomponent metallic melts, the effect of each component on the melt's adhesion to the solid phase, and the structure and phase composition of the products of melt interaction with carbon and their distribution are discussed; the effect of a change in thermodynamic properties of the Cr-subgroup metals in the Ni melt on the character of contact interaction in the solid-liquid system is examined, and attention is focused on the effect of a change in the isobaric-isothermal potential of the metal reaction with C and the thermodynamic activity of the adhesion-active component on the wettability and structure of the interface area between graphite and the metallic melt. The degree of wettability is determined by the sessile drop method in a 2 x 10^{-3} Pa vacuum using separate heating of the metal alloy and graphite substrate. The concentrational dependence of graphite wettability by Ni-Cr, Ni-Mo, and Ni-W melts at 1,773K and the constitution diagram of the Ni-W-C system and the dependence of the wetting angle on the W concentration in the Ni melt are plotted. The microstructure of the contact interaction zones of the above systems is shown. The findings make it possible to arrange the Cr-subgroup metals into a Cr-Mo-W series in the increasing order of adhesion in the Ni melt and show that the course of the isothermal wetting curve depends on the phase formation on the contact boundary. The relationship of the capillary properties of the interface and the isobaric-isothermal potential is analyzed. The experiment method has a greater effect on the capillary characteristics of the system than on the structure and phase composition of the interface. The authors are grateful to V.G. Delevi for assistance with X-ray studies. Figures 4; references 4.

Formation of Residual Stresses During the Laser Heat Treatment of CrVMn Steel

937D0099A Moscow FIZIKA I KHIMIYA OBRABOTKI MATERIALOV in Russian No 1, Jan-Feb 93 (manuscript received 5 Aug 92) pp 31-38

[Article by D.M. Gureyev, Samara; UDC 539.4.04.13:535.211]

[Abstract] Specimens of CrVMN low-alloy tool steel were studied to identify the basic laws governing the formation of residual stresses in the surface layers of zones affected by laser heat treatment as the parameters of the laser treatment process are varied. The steel studied contained the following (percent): C, 0.9 to 1.0; Cr, 0.9 to 1.2; W, 1.2 to 1.6; Mn, 0.8 to 1.0; and Si, 0.15 to 0.35. Pieces of steel 5 and 15 mm thick were first subjected to standard bulk heat treatment: heating to 650-700°C, hardening in oil from 830 to 850°, and one-time tempering at 150-200° to a hardness of 60-61 HRC and at 200-300°C to a hardness of 53-54 HRC. An LGN-702 continuous-wave CO_2 laser and a Kvant-15 pulsed neodymium laser were used for the heat treatment. The laser beam was focused on a strip 10 x 1 mm with the power density distributed evenly along the length of the strip. The speed at which the beam was moved was varied between 0.7 and 7.0 mm/s. Before the laser treatment began, an absorbent coating (i.e., a layer of black typographic paint about 40 µm thick) was applied to the surface of each test specimen. The laser pulse did not exceed 17 J, and pulses lasted 5 ms in most cases. The $\sin^2\Psi$ method was used along with a Strainflex PSF-2M unit to measure the residual stresses, a DRON-3.0 diffractometer was used to perform X-ray phase analyses, and Neophot-30 and PMT-3 microscopes were used to perform metallography and microdurometry studies. An interconnection between the magnitude and size of the residual stresses formed and the steel's structural composition was discovered. Specifically, changes in the hardness and stressed state of the test specimens' surfaces were noted. Figures 6, tables 2; references 4: Russian.

Phase and Structural Transformations in Steels During Gas Thermal Spraying of Coatings

937D0099F Moscow FIZIKA I KHIMIYA OBRABOTKI MATERIALOV in Russian No 1, Jan-Feb 93 (manuscript received 11 Jun 92) pp 77-83

[Article by V.N. Antsiferov, A.M. Shmakov, and M.V. Ivanova, Perm; UDC 621.793.7]

[Abstract] The phase and structural transformations occurring in cast and powder steels coated by the method of gas thermal spraying were studied. Special attention was paid to the physicochemical processes occurring in the transition zone as a result of the energy factors associated with the spraying process. Samples of sintered powder steels containing different amounts of carbon (SP-20, SP-35, SP-60, SP-80, and SP-90) and alloy-forming elements (SP-Kh5, SP-80Kh5, SP-40N, and SP-Kh18N9T) with a porosity of 10-12 percent and their cast analogues were used for the experiments. Aluminum and molybdenum coatings were applied to some of the steel specimens on a KDM-2 unit in either one pass for a single-layer coating or by continuous spraying to achieve coatings 400 to 600 µm thick. Nickel-aluminum and bronze plasma coatings of PTYu5N and BrOF-10 powder were applied to other specimens on a UPU-ZD unit. The steels were subjected to chemical analysis by the coulometry method on a Kulomatik-S, analysis of the elemental composition on an MAR-2M, structural examination under Epignost and Neofot-21 microscopes and a PMT-3 microhardness tester, and layer-by-layer phase analysis on DRON-2 and DRON-3M diffractometers. A ZM tensile testing machine was used to test the specimens' cohesive strength. The metallographic analysis conducted confirmed that a heat-affected zone may be established in the structure of the transition region in each specimen. The parameters of this zone are linked to the coating application method, type of material sprayed, preheating temperature, and content of alloy-forming elements in the steels. When a single layer of molybdenum is sprayed onto a preheated substrate of SP90-2, the width of the heat-affected zone increases at temperatures between 20 and 350°C, then moderates, and eventually disappears completely at 400-500°C. No heat-affected zone was located in cases of electric arc spraying of aluminum, in plasma spraying of bronze, or in the absence of preheating. A heat-affected zone was very evident in the steel specimens subjected to electric arc spraying with molybdenum or plasma spraying of the powder PTYu5N (which reacts to heat). The powder steels were more inclined to form heat-affected zones than the cast specimens were. The structure and phase composition of the heat-affected zones formed were found to affect the coatings' stressed state and cohesive strength. The experiments also established that maximum cohesive strength is obtained when a ferrite or austenite structure of the steel base's surface is achieved. Figures 2, tables 6; references 8: Russian.

Increasing the Wear- and Corrosion Resistance of Copper by Electrospark Alloying

937D0099G Moscow FIZIKA I KHIMIYA OBRABOTKI MATERIALOV in Russian No 1, Jan-Feb 93 (manuscript received 19 Feb 92) pp 101-106

[Article by A.I. Mikhaylyuk, V.G. Revenko, and N.N. Natarov, Kishinev, 19 Feb 92; UDC 669.3:669.84]

[Abstract] A study examined the possibility of improving the wear- and corrosion-resistance of copper by electrospark alloying with aluminum and graphite electrodes. Six samples of copper were subjected to electrospark alloying on an Elitron-22 unit. The process parameters were varied in each case. M-1 copper, EG-2 graphite, A95 aluminum, and a combination of A95 aluminum and EG-2 graphite were all tested as electrodes. The working current and electrospark alloying discharge energy were also varied. The electrospark-alloyed copper samples were subjected to X-ray phase analysis and wear and corrosion resistance tests. The tests established that the formation of $CuAl_2$ and $Cu_{0.6}Al_{0.4}$ intermetallide phases in the surface layer of copper significantly increases the effect of hardening due to the thermoplastic deformation accompanying the electrospark alloying process. The combination of the hardening and solid-lubrication effects of the formation of the aforesaid intermetallides and free graphite increased the copper test specimens' wear resistance when subjected to dry friction by almost an order of magnitude and increased wear resistance when subjected to the friction of boundary lubrication by two orders of magnitude. The formation of protective surface layers (including intermetallides and oxides) that

occurred during electrospark alloying resulted in a significant improvement in the corrosion resistance of copper test pieces subjected to sea water and industrial atmospheres. Figures 5, table 1; references 5: Russian.

Surface Fracture of Brittle Materials During Thermal Shock

937D0100C Moscow FIZIKA I KHIMIYA OBRABOTKI MATERIALOV in Russian No 2, Mar-Apr 93 (manuscript received 24 Sep 92) pp 53-58

[Article by N.A. Bochkov and V.S. Yegorov, Luch Scientific Research Association, Podolsk; UDC 536.495:539.4.014]

[Abstract] A study examined the fracture of ZrC disks due to thermal shocks in a tin melt and to local electron beam heating. The study $ZrC_{0.97}$ disks, which were made by semidry molding and subsequent sintering, measured 46 x 3 mm^2 and 58 x 8 mm^2. The disks contained the following (mass percent): zirconium, 86.2; bound carbon, 11; free carbon, 0.1; nitrogen, 0.02; oxygen, 1.3; and other impurities, <0.05. The disk material had a porosity of 4 to 6 percent, resistivity of 0.66 μO-m, flexural strength of 230 MPa (with a variance of 10 percent), compression strength of 870 MPa (variance, 9 percent) at room temperature, and compression strength of 970 MPa (variance, 7 percent) at 1,000°C. It had a Young modulus of 350 GPa, Poisson coefficient of 0.2, and average coefficient of linear expansion of 6 x 10^{-6} K^{-1}. The study disks (with their faces insulated by a 10-mm asbestos layer) were heated by immersing them in tin heated to a specified temperature (25 to 50°C) for a specified time (measured within 0.01 s). The stress field in the tin melt-heated disks was found to have a zone of extension in the center of the specimen and a zone of compression in their peripheral regions. Local heating gives rise to a much more complex and nonuniform stress field characterized by intensive compression at the heating spot and a zone of maximum tensile stresses that changes its location over time. In cases of short heating times ($t < 0.02$ s), the tensile stress zone is three-dimensional and located on the disk axis under the compression zone. In cases of longer heating times ($t > 0.4$ s), the said zone extends to the irradiated surface. The magnitudes of the maximum tensile and compressive stresses in both instances of thermal loading change at different rates and reach their extrema at different points in time. Their ratios vary within broad bounds and attain huge values with small thermal effect durations. In cases of local heating with a heat flux exceeding 5 kW/cm^2 and pulse lengths not exceeding 0.005 s, the material in the heating zone breaks through to a depth of several tens of microns. As in the case of fracture due to tensile stresses, the limiting loads during fracture in the compression zone depend on the gradient of the compressive stresses. Figures 2, tables 2; references 7: Russian.

Performance of Belbor Cutters During Machining of Hardened Steel

937D0104D Kiev SVERKHTVERDYYE MATERIALY in Russian No 2 (83), Mar-Apr 93 pp 44-47

[Article by V.I. Shemegon, Far Eastern Scientific Research Institute of Shipbuilding Engineering, Khabarovsk; UDC 621.9.02:669.245]

[Abstract] The expanding use of boron nitride-based polycrystal superhard materials in the tool-making industry prompted an investigation into the performance of Belbor cutters during the machining of hardened steels with various chemical compositions. The Belbor cutter serviceability is examined in two stages: by turning samples from high-speed hardened steel R6M5 (with HRC=62-64) with a 30 mm diameter and by boring samples from hardened tool steel U8A (with HRC=59-62) with a 36 mm diameter. These steels are selected due to their frequent use in tool-making. The dependence of the cutter resistance T and L on the cutting speed and the dependence of the flank wear land—the wear criterion—on the machining duration are plotted. The effect of the cutting sped on the Belbor cutter wear rate and the crater dimensions on the cutting edge during the machining of hardened steel is summarized. The findings demonstrate that Belbor tools used for hardened steel machining have a high resistance and serviceability within a narrow cutting speed range; as the cutting speed is decreased or increased, both parameters deteriorate because the tool wear characteristics change. The optimum turning and boring speeds are 23.6 and 35.6 m/min, respectively. Figures 5; tables 1; references 3.

Me-X Centers in Synthetic Diamonds

937D0105A Kiev SVERKHTVERDYYE MATERIALY in Russian No 1 (82), Jan-Feb 93 pp 7-11

[Article by V.G. Malogolovets, S.A. Ivakhnenko, G.V. Chipenko (deceased), Superhard Materials Institute at the Ukrainian Academy of Sciences, Kiev; UDC 535.3:666.233]

[Abstract] The use of infrared spectroscopy to estimate the composition and impurity concentration in synthetic diamonds and the correlations used for this purpose are discussed, and it is noted that the Me-X impurity center which is reflected in infrared spectra by additional absorption bands within the 500 and 900 cm^{-1} region cannot be assessed by traditional methods. The position and shape of these absorption bands in the absorption bands of crystals grown in different systems attest to the role of transition metal (Fe group) atoms used to synthesize the diamonds in the impurity center formation. The infrared absorption spectra of Iv pure synthetic diamonds and diamonds with additional absorption spectra in the 500 and 900 cm^{-1} region, the infrared absorption spectra of Iv single crystals and diamonds with Me-X centers before and after heat and pressure treatment, and the correlations between the line strength due to the A-centers in the spectra of heat and pressure treated crystals with the line strength due to the C-centers in the spectra of the original samples and between excess absorption at a 1,282 cm^{-1} wavelength with the 870 cm^{-1} line strength due to the Me-X centers are plotted. The findings confirm the nitrogen origin of the Me-X impurity centers and make it possible to derive an expression which reflects the dependence of the 870 cm^{-1} absorption line strength due to these centers on their concentration in the crystals. These findings also facilitate the study of the functional relationship between the atomic impurity concentrations of the solvent metal in synthetic diamonds and other crystal properties. Figures 3; references 9: 6 Russian, 3 Western.

Investigation of Mechanical Properties of Carbonado Polycrystal Diamonds

937D0105B Kiev SVERKHTVERDYYE MATERIALY in Russian No 1 (82), Jan-Feb 93 pp 24-26

[Article by O.Ch. Kozhogulov, K.Kh. Khaydarov, V.I. Malnev, Physics Institute of the Republic of Kyrgyzstan, Bishkek, and Superhard Materials Institute at the Ukrainian Academy of Sciences, Kiev; UDC 539.411.531:666.233]

[Abstract] The mechanical properties of carbonado polycrystal diamonds (ARK) which were synthesized for six years at the Tokmak plant are studied; to this end, the initial cylindrical samples with a 4 mm diameter and 3-4 mm height are chemically cleaned to remove the solvent metal and graphite. The samples' phase composition is examined by X-ray phase analysis in a DRON-2 unit. Diffraction patterns of an ARK diamond are plotted, and electron microscope pictures of the polished and cleaved surfaces of an ARK diamond are cited. The hardness and crack resistance of diamonds is measured within a broad temperature range, and the samples are divided into three categories according to their synthesis time within the six-year period. The findings show that at room temperature, the sample microhardness roughly corresponds to that of similar diamonds and is commensurate with the hardness of single crystal natural and synthetic diamonds (approximately 85 GPa). At elevated temperatures, the ARK diamond hardness is also commensurate with that of single crystal natural and synthetic diamonds while at a temperature of 1,200K or above, ARK diamonds crack intensively, probably due to stresses resulting from a difference in the thermal expansion coefficients of the matrix and metal inclusions. The dynamic strength of ARK diamonds is also measured. In all, polycrystal diamonds have sufficient mechanical properties and may ensure good performance of machine tools. Figures 2; tables 3; references 4.

Study of Feasibility of Acoustic Testing of Kiborite Tools

937D0105C Kiev SVERKHTVERDYYE MATERIALY in Russian No 1 (82), Jan-Feb 93 pp 41-43

[Article by N.S. Ipatov, V.N. Makarov, L.S. Paokina, S.L. Proskuryakov, L.Ya. Slavina, Rybinsk Aviation Engineering Institute; UDC 658.562:621.9.02]

[Abstract] The use of kiborite—a cubic boron nitride-based superhard polycrystalline material—for making cutting inserts for high-speed turning is discussed, and kiborite's broad spread of wear resistance indicators is noted. This spread substantially limited the material's applications and prompted an investigation into the feasibility of nondestructive testing of ready tools, particularly acoustic testing. To check the possibility of acoustic testing, 135 kiborite cutter insert samples with a 7 mm diameter and 4 mm height are examined; the sample density is determined by measuring the linear dimensions accurately within 1 μm and the mass—accurately within 0.1 mg. The elastic longitudinal vibration propagation speed is measured in a test unit where the sample is placed between two piezoelectric transducers and ultrasonic electric oscillations generated by an oscillator are transformed into the mechanical vibrations transmitted to the sample, converted by the pickup, and measured by a Zvuk-107 instrument. The spread field of the sample density and acoustic vibration propagation speed, the dependence of the cutting force components and tool wear on the density and vibration propagation velocity, and the dependence of the tool resistance on the vibration propagation velocity are plotted. The sample wear is examined by turning blanks of the same length. The findings demonstrate that the cutting insert density cannot be used as a diagnostic variable, but the elastic vibration propagation speed is closely related to the cutting forces, wear, and resistance; as the propagation speed increases, the cutting force and tool wear decrease while the tool resistance rises. Acoustic testing is recommended for obtaining stable operating indicators during machining of superalloys, and it is suggested that the cutting inserts be divided into three categories according to the propagation velocity: 15.0+/-0.5, 15.75+/10.25, and 16.25+/10.25 km/s for machining small and large surfaces of noncrucial parts and large surfaces of crucial parts, respectively. Figures 3; references 3.

Computer-Aided Diamond Drill Design

937D0105D Kiev SVERKHTVERDYYE MATERIALY in Russian No 1 (82), Jan-Feb 93 pp 48-51

[Article by A.A. Stepanov, St. Petersburg Mechanical Institute; UDC 621.95.025.7:666.23.668.9]

[Abstract] Increasing uses of diamond drills for making holes in glass-and boron-based plastics, including nickel binder-based drills manufactured by electroplating, prompted a study of computer-aided design of diamond drills consisting of two parts: a metal mandrel and a diamond-bearing layer applied to it. The diamond powder grade (AS6, AS15, AS20, etc.) is selected based on an analysis of the economic efficiency of the drilling process and available stocks of diamond raw materials. The effect of the diamond powder granularity on the process yield, tool service life, and the resulting surface quality is discussed. An engineering procedure developed for determining the diameter and linear dimensions of the diamond drill mandrels is outlined, and the relevant computer software is described. The software is compiled in the Fortran language and can run on mainframes or microcomputers; the type of the composite drilled, the hole diameter, type, and accuracy class, the total drilling length or the necessary number of holes and their length, the requisite surface quality, the spindle power and rotation speed, radial beats, and available diamond stocks are used as the source data. A block-diagram of the diamond drilling operation analysis is cited. The program makes it possible quickly and reliably to solve the issues of diamond drill design and ensure process preparation; it can be realized for any composite, provided that experimental data on its machinability are available. Figures 2; references 3.

Effect of Diamond Grinding Method on Residual Stresses in VT14 Titanium Alloy

937D0105E Kiev SVERKHTVERDYYE MATERIALY in Russian No 1 (82), Jan-Feb 93 pp 55-59

[Article by P.G. Matyukha, V.P. Tsokur, Donetsk Polytechnic Institute; UDC 621.923]

[Abstract] The negative effect of the high thermal activity, tendency to contact setting under friction, and low thermal conductivity of titanium alloys on the machined surface

quality and the feasibility of overcoming these problems by using diamond grinding are outlined, and the effect of the grinding method and grinding wheel granularity and diamond grade on first-kind residual stresses in the VT14 titanium alloy is investigated. To this end, samples are subjected to surface grinding by various methods in a mod. 3G71 machine using diamond wheels from AS6 and ARV diamonds with and without electric current applied to the grinding zone. Identical grinding wheel surface conditions are ensured at the start of each operation by dressing and truing. The surface layer is pickled, and sag measurements are taken in a PION-2 unit. The first-kind residual stress distribution in the surface layer depth of the VT14 titanium alloy under regular diamond grinding, grinding with electric discharge truing, and diamond electric discharge grinding with AS6 and ARV grinding wheel is plotted. The study shows that residual tensile stresses develop at a 5 μm depth; diamond electric discharge grinding is characterized by the highest stress. ARV wheels develop residual tensile stresses up to a depth of 120 μm and are therefore unsuitable for grinding the VT14 alloy; it is recommended that the alloy be machined by diamond grinding with electric discharge truing with periodic electric discharge dressing in the autonomous zone. The diamond granularity has the greatest effect on the residual stress under diamond electric discharge grinding. Figures 3; references 3.

END OF FICHE DATE FILMED

12 JULY 1993